OPEN

Spectrum of the Breast Lesions With Increased ^{18}F-FDG Uptake on PET/CT

Aisheng Dong, MD, Yang Wang, MM,† Jianping Lu, MD,‡ and Changjing Zuo, MD**

Abstract: Interpretation of ^{18}F-FDG PET/CT studies in breast is challenging owing to nonspecific FDG uptake in various benign and malignant conditions. Benign conditions include breast changes in pregnancy and lactation, gynecomastia, mastitis, fat necrosis, fibroadenoma, intraductal papilloma, and atypical ductal hyperplasia. Among malignancies, invasive ductal carcinoma and invasive lobular carcinoma are common histological types of breast carcinoma. Rarely, other unusual histological types of breast carcinomas (eg, intraductal papillary carcinoma, invasive micropapillary carcinoma, medullary carcinoma, mucinous carcinoma, and metaplastic carcinoma), lymphoma, and metastasis can be the causes. Knowledge of a wide spectrum of hypermetabolic breast lesions on FDG PET/CT is essential in accurate reading of FDG PET/CT. The purpose of this atlas article is to demonstrate features of various breast lesions encountered at our institution, both benign and malignant, which can result in hypermetabolism on FDG PET/CT imaging.

Key Words: breast, neoplasm, FDG, PET/CT, CT

(*Clin Nucl Med* 2016;41: 543–557)

Imaging diagnostic evaluation of the primary breast lesion itself is mainly determined from mammography, ultrasound, and MRI. In patients with known breast carcinoma, FDG PET/CT is performed for detection of unsuspected extra-axillary lymph nodes and distant metastases and evaluation of response to therapy. It is a problem-solving method when results of conventional imaging are equivocal.[1] Breast incidental hypermetabolic lesions on FDG PET/CT are reported in 0.36% to 1.01% of female patients, and the prevalence rate of malignancies is approximately 27% to 38%.[2–4] The false-positive interpretations may result from etiologies including benign hyperplasia, benign tumor, inflammation, and infection. Therefore, breast incidental hypermetabolic lesions need further workup, usually mammogram and/or ultrasound, and possible biopsy.[2–4] At our institution, we encountered ^{18}F-FDG PET/CT scans that demonstrated a variety of breast lesions with hypermetabolism. The purpose of this atlas article is to demonstrate a spectrum of breast lesions, both benign and malignant, which can show increased FDG uptake on PET/CT imaging. In addition, available radiological and pathological images are presented in this article because familiarity with the imaging features of different imaging modalities is helpful for making differential diagnosis and knowledge of the pathological characteristics of the breast lesions is helpful for understanding the mechanisms of FDG uptake.

Received for publication January 19, 2016; revision accepted January 20, 2016.
From the Departments of *Nuclear Medicine, †Pathology, and ‡Radiology, Changhai Hospital, Second Military Medical University, Shanghai, People's Republic of China.
Aisheng Dong and Yang Wang contributed equally to the article.
Conflicts of interest and sources of funding: none declared.
Correspondence to: Changjing Zuo, MD, Department of Nuclear Medicine, Changhai Hospital, 168 Changhai Road, Yangpu District, Shanghai 200433, People's Republic of China. E-mail: 836993813@qq.com; or Jianping Lu, MD, Department of Radiology, Changhai Hospital, 168 Changhai Road, Yangpu District, Shanghai 200433, People's Republic of China. E-mail: cjr.lujianping@vip.163.com.

ISSN: 0363-9762/16/4107–0543
DOI: 10.1097/RLU.0000000000001203

DISEASES OF THE FEMALE BREAST

Normal Breast

The physical FDG uptake of normal breast tissues is generally homogeneous with SUV_{max} lower than 2.5.[5–7] Factors that affect FDG uptake of normal breast tissue are mammographic density, age, and menstrual cycle. Breast FDG uptake significantly decreases as breast density decreases[5–7] and age increases.[7] In fertile female patients, FDG uptake of the normal breasts shows changes according to the menstrual cycle. The breast tends to show higher FDG uptake in the secretory, flow, and ovulatory phases than that in proliferative phase.[8,9] Menopausal status has no significant effect on FDG uptake of normal breast.[5,7] FDG uptake of the normal breast tissue has either no change or decrease on dual time point FDG PET.[10] Therefore, dual time point FDG PET is helpful for detection of the breast malignancy by increasing the contrast between the lesion and the surrounding background. The FDG uptake of the bilateral beasts is usually symmetrical. Rarely, the bilateral beast FDG uptake may be asymmetrical which may be due to difference in response to hormonal stimulation (Fig. 1).

Breast During Pregnancy and Lactation

During pregnancy, the breast undergoes numerous changes in response to an increase in circulating hormones. These changes are characterized by marked ductular sprouting, increase in glandular vascularity, marked lobular growth with cellular proliferation, and involution of the fibrofatty stroma.[11] These changes are more notable during lactation, the secretory state. Glucose plays a major role in mammary gland function during lactation as it is used both as a fuel and as a precursor of milk components.

Pregnant and postpartum women require FDG PET/CT examinations in very few cases, such as evaluation for malignant tumors. During pregnancy, the FDG uptake of the enlarged breast may, or may not, be similar to liver (Fig. 2).[12] At CT, lactating breasts show enlargement with bilateral cord- and mass-like hyperattenuating tissue. Lactating breasts used for feeding can show diffuse and intense FDG uptake (Fig. 3), whereas lactating breasts unused for feeding only show little FDG uptake (Fig. 4).[13,14] Therefore, suckling may be an important stimulus for FDG uptake in the lactating breasts by increasing expression of the insulin-independent glucose transporter (GLUT).[15] The influence of breastfeeding on breast FDG uptake should be taken into consideration when interpreting FDG PET/CT findings in the postpartum women.

Mastitis

Mastitis is classified into 3 main types: infectious including simple mastitis (eg, lactational and nonlactational), complicated mastitis (eg, infected cysts, infected galactoceles, infected hamartoma, and infected hematoma), and specific mastitis (eg, tuberculosis); noninfectious (eg, periductal mastitis, plasma cell mastitis, granulomatous mastitis, and diabetic mastopathy); and malignant

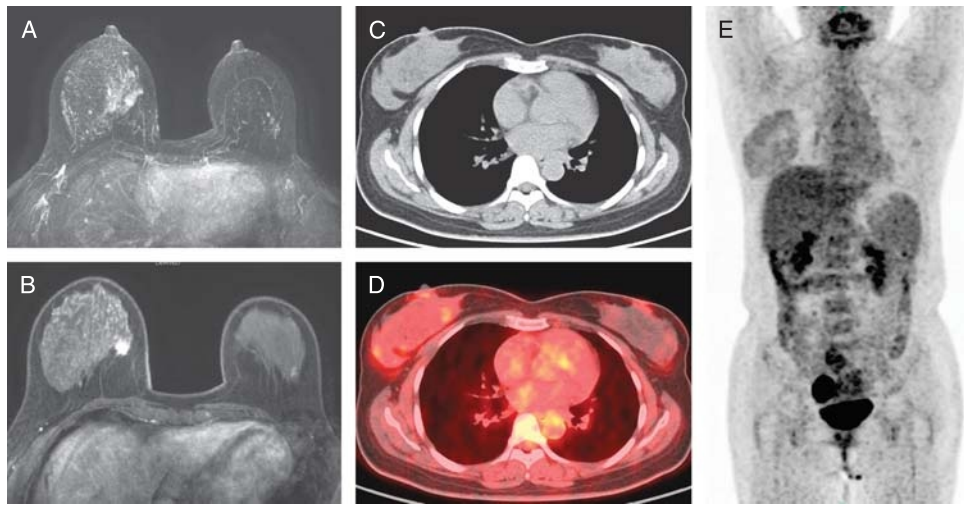

FIGURE 1. A 44-year-old woman with right breast pain for 15 days. Maximum intensity projection (MIP) enhanced T1-weighted MR (**A**) and transverse enhanced T1-weighted MR images (**B**) showed enlargement of the right breast with stippled and patchy enhancement. FDG PET/CT was performed during flow phase of the menstrual cycle. Transverse CT (**C**), corresponding fused (**D**), and MIP PET (**E**) images showed diffusely increased FDG uptake of the right breast with SUV_{max} of 2.0. The left breast had no significantly increased FDG uptake. Fine needle aspiration of the right breast revealed benign hyperplasia.

mastitis (eg, inflammatory breast carcinoma and malignant breast abscess).[16] Infectious mastitis is more common during the childbearing period especially during lactation. Noninfectious mastitis encompasses a group of aseptic or chemical inflammatory breast disorders. Malignant mastitis is the most serious form of mastitis, usually accompanying the inflammatory breast carcinoma. Clinically, inflammatory breast carcinoma is characterized by the rapid onset of swelling and enlargement of the breast. Differentiating this disease from acute mastitis may be difficult at presentation. Inflammatory breast carcinoma typically occurs in older women, whereas acute mastitis usually affects younger, lactating women.[16]

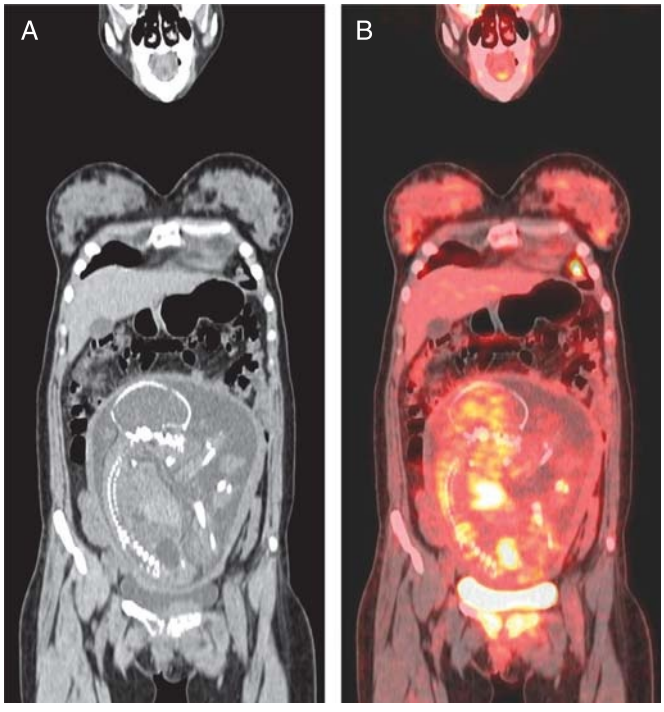

FIGURE 2. A 22-year-old pregnant woman with disseminated malignant tumor at 30-week gestation. Coronal CT (**A**) and corresponding fused (**B**) images showed diffusely increased FDG uptake of the bilateral breasts with SUV_{max} of 3.0.

Increased FDG uptake in acute or chronic mastitis caused by bacteria, virus, parasite, tuberculosis, siliconoma, and surgery has been reported in the literature.[17–24] Acute mastitis can show diffuse FDG uptake (Fig. 5). Chronic lesions usually show focal FDG uptake (Figs. 6 and 7). Inflammatory breast carcinomas demonstrate diffuse or focal FDG uptake in the enlarged breasts with increased skin FDG uptake.[25]

Fat Necrosis

Fat necrosis is a sterile, inflammatory process which results from aseptic saponification of fat by means of blood and tissue lipase. It belongs to noninfectious mastitis. It varies in appearance depending on the stage of the process. Histologically, it is characterized as fat-filled macrophages and foreign body giant cells surrounded by interstitial infiltration of plasma cells.[26] The common etiological factors of breast fat necrosis include trauma, biopsy, surgery, and radiotherapy.

On mammography, fat necrosis can present as lipid cysts, coarse calcifications, focal asymmetries, microcalcifications, or speculated masses. Fat necrosis can result in increased FDG uptake because of the presence of metabolically active inflammatory cells (Fig. 8).[27–29]

Atypical Ductal Hyperplasia

Atypical ductal hyperplasia is a neoplastic intraductal lesion characterized by proliferation of evenly distributed, monomorphic cells and associated with an elevated risk for progression to invasive

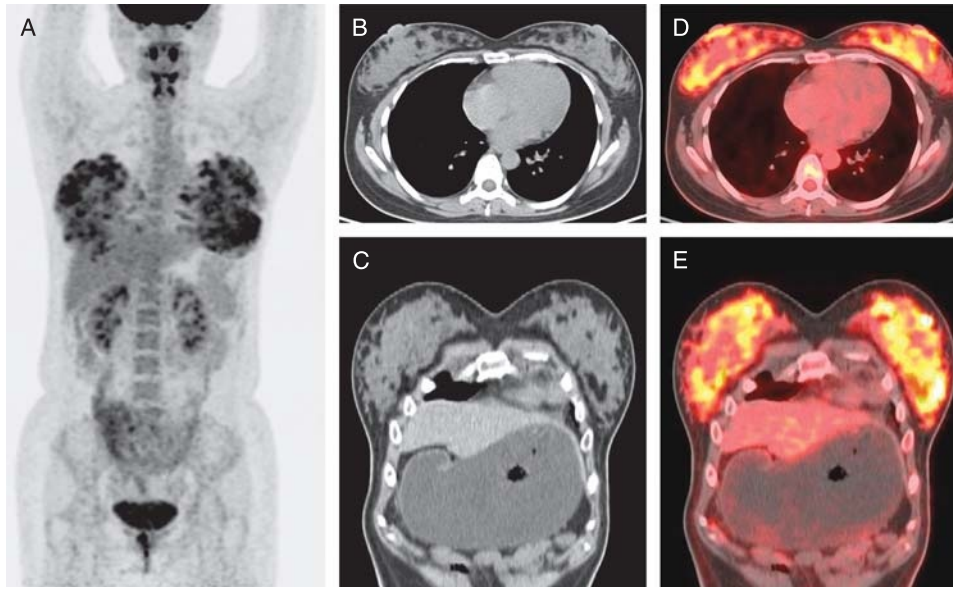

FIGURE 3. A 27-year-old woman with bilateral breast-feeding at 2 months postpartum. MIP PET (**A**), transverse (**B**) and coronal (**C**) CT, and corresponding fused (**D**, **E**) images showed symmetrically enlarged breasts with diffuse intense FDG uptake (SUV_{max}, 8.0).

breast carcinoma.[30,31] It is more often found in older women and an unusual finding in the adolescent and young adult female patients. FDG PET/CT findings of atypical ductal hyperplasia have been rarely reported. We presented a case of atypical ductal hyperplasia showing focal FDG uptake with SUV_{max} of 6.3, which mimicked breast carcinoma (Fig. 9). On CT, the lesion could not be detected in the dense breast tissue.

FIGURE 4. A 30-year-old woman at 2 months postpartum who stopped breast-feeding for 1 month. MIP PET image showed diffuse FDG uptake of the bilateral breasts with SUV_{max} of 3.2.

Fibroadenoma

Fibroadenoma is the most common benign breast tumor with admixture of stromal and epithelial proliferation, occurring most frequently in women of child-bearing age.[31] Fibroadenoma usually presents as a painless, solitary, firm, slowly growing, mobile, well-defined nodule. It can be multiple in the same or in both breasts and may grow very large mainly when it occurs in adolescents.

At CT, fibroadenomas appear as well-circumscribed, round, or oval masses that may demonstrate coarse popcorn-like calcifications.[32] FDG PET provides a high accuracy in the differentiation of fibroadenomas from malignant tumors because fibroadenomas usually show no or mild FDG uptake. Rarely, fibroadenomas may show significantly higher FDG uptake than the normal breast tissue and mimic malignancies (Fig. 10).[33,34]

Intraductal Papillary Neoplasms

Papillary neoplasms are characterized by epithelial proliferations supported by fibrovascular stalks. They may occur anywhere within the ductal system from the nipple to the terminal ductal lobular unit and may be benign (intraductal papilloma), atypical, or malignant (intraductal papillary carcinoma).[31] These neoplasms can be either solitary and central in location or multifocal within the terminal ductal lobular unit. The differentiation of benign from malignant papillary neoplasms on imaging is often difficult because of the wide spectrum of appearances of these lesions on MRI, ultrasound, and mammography.[35]

Intraductal Papilloma

Overall, less than 10% of benign breast neoplasms correspond to intraductal papillomas.[31] Intraductal papilloma can show slight (similar to the liver) or high FDG uptake.[36–38] It is unclear whether the FDG uptake degree of intraductal papillomas is related to the GLUT subtypes or hexokinase II expression. Complex cyst with hypermetabolic mural nodule may suggest the diagnosis (Fig. 11).

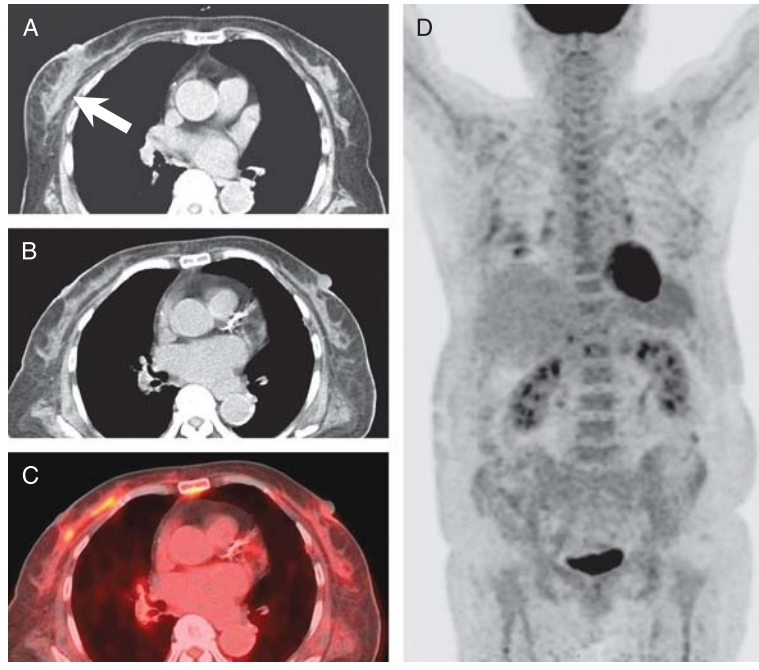

FIGURE 5. A 81-year-old woman with right breast pain for 3 days. Chest CT (**A**) showed enlargement of right breast with thickened skin and misty fat tissue (arrow). Fine needle aspiration of right breast revealed simple infectious mastitis. Fifteen days after antibiotic treatment, transverse CT (**B**), corresponding fused (**C**), and MIP PET (**D**) images showed inhomogeneous FDG uptake of the right breast with SUV_{max} of 4.5.

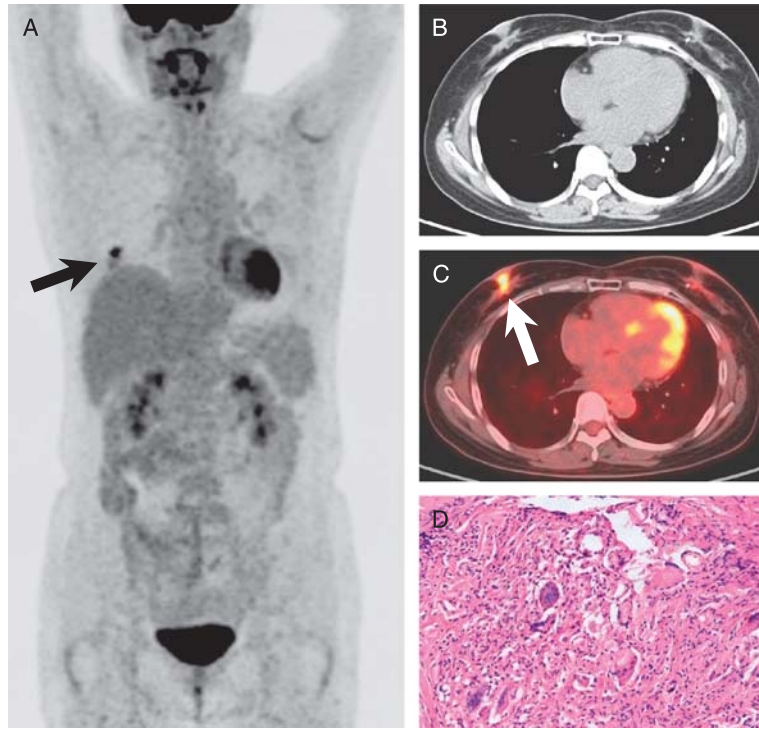

FIGURE 6. A 53-year-old woman with a history of right breast surgery for benign lesion. MIP PET (**A**), transverse CT (**B**), and corresponding fused (**C**) images showed focal FDG uptake with SUV_{max} of 7.2 in the right breast (arrows). The patient underwent resection of the lesion. Photomicrograph (**D**) revealed foreign body granuloma (hematoxylin-eosin stain; original magnification, ×200).

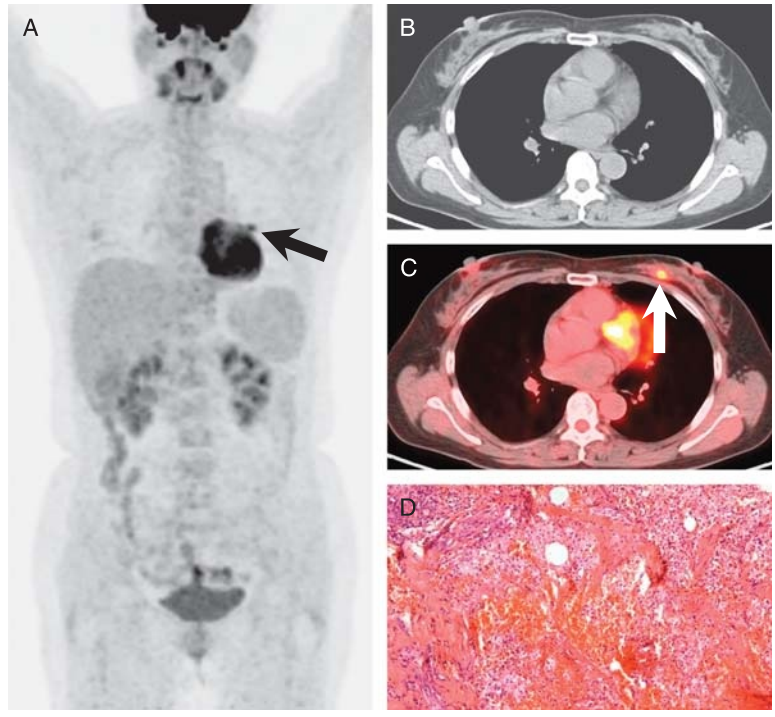

FIGURE 7. A 53-year-old woman who incidentally found a nodule in her left breast 1 week ago. MIP PET (**A**), transverse CT (**B**), and corresponding fused (**C**) images showed a FDG-avid nodule with SUV_{max} of 5.7 in the left breast (arrows). The patient underwent resection of the lesion. Photomicrograph (**D**) revealed ruptured duct with hemorrhage and inflammation (hematoxylin-eosin stain; original magnification, ×100).

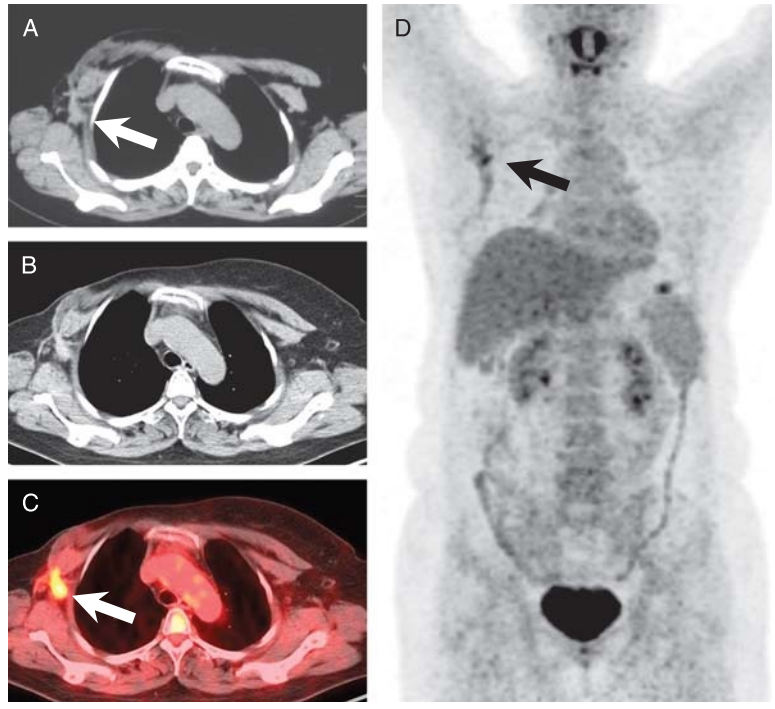

FIGURE 8. A 50-year-old woman who underwent right breast carcinoma resection 15 months ago. Follow-up chest CT (**A**) 6 months after operation showed a hyperdense spiculated lesion (arrow) in the right axilla. Nine months later, transverse CT (**B**), corresponding fused (**C**), and MIP PET (**D**) images showed intense FDG uptake with SUV_{max} of 5.2 of the lesion (arrows). The size of the lesion had no change. Fine needle aspiration of the lesion revealed necrotic fat cells and foamy cells, which were consistent with fat necrosis.

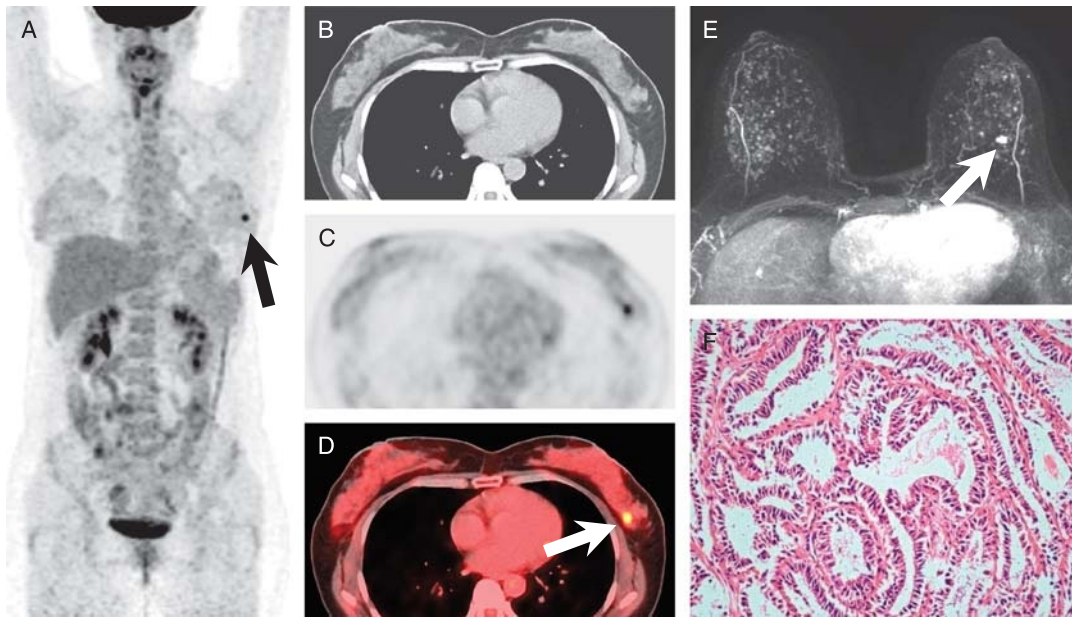

FIGURE 9. A 48-year-old woman with left breast pain for 2 weeks. MIP PET (**A**), transverse CT (**B**), corresponding PET (**C**), and fused (**D**) images showed a FDG-avid nodule with SUV_{max} of 6.3 in the left breast (arrows). MIP enhanced T1-weighted MR image (**E**) showed remarkable enhancement of the nodule (arrow). The patient underwent resection of the lesion. Photomicrograph (**F**) revealed atypical ductal hyperplasia (hematoxylin-eosin stain; original magnification, ×200).

Intraductal Papillary Carcinoma

Less than 2% of breast carcinomas correspond to intraductal papillary carcinomas.[31] Intraductal papillary carcinoma has a very favorable prognosis. Information is limited regarding the FDG PET/CT features of intraductal papillary carcinomas. We presented a case of intraductal papillary carcinoma located in the subareolar region, showing high FDG uptake (Fig. 12).

Ductal Carcinoma In Situ

Ductal carcinoma in situ (DCIS) is a neoplastic intraductal lesion characterized by increased epithelial proliferation, subtle to marked cellular atypia and an inherent but not necessarily obligate tendency for progression to invasive breast carcinoma.[31] With improvements in imaging and increasing of screening, the detection of DCIS has been increasing. The most common mammographic

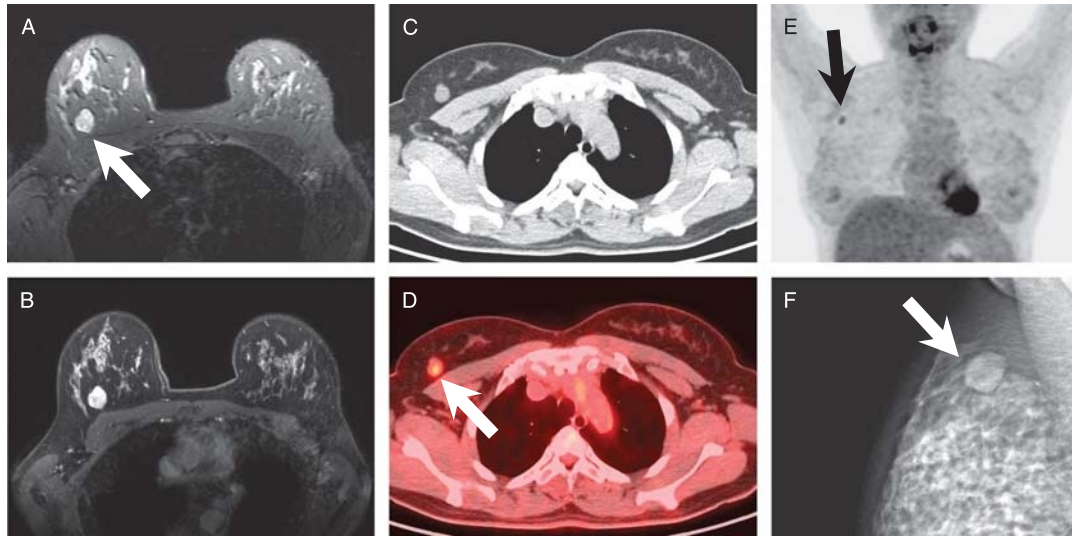

FIGURE 10. A 42-year-old woman with a 30-day history of left breast pain. Transverse T2-weighted MR image (**A**) showed a well-circumscribed round nodule with hyperintensity in the right breast (arrow). Enhanced T1-weighted MR image (**B**) showed remarkable enhancement of this nodule. Transverse CT (**C**), corresponding fused (**D**), and MIP PET (**E**) images showed increased FDG uptake of this nodule with SUV_{max} of 2.5 (arrows). One year later, a follow-up right mediolateral mammogram (**F**) revealed a well-circumscribed, round-shaped hyperdense nodule (arrow) in upper outer quadrant of the right breast. The patient underwent resection of the nodule. Photomicrograph revealed fibroadenoma.

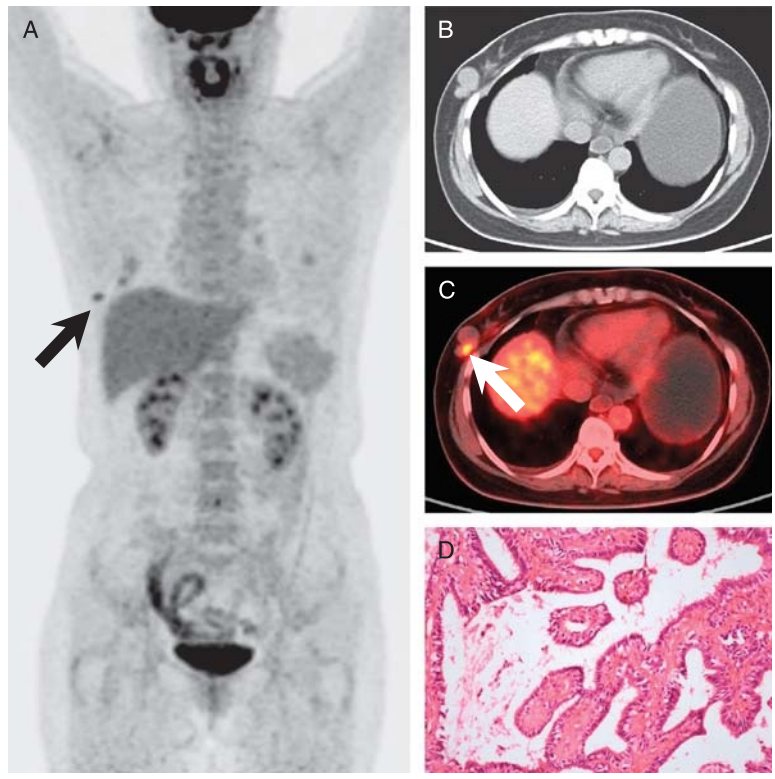

FIGURE 11. A 54-year-old woman with resection of right breast fibroadenoma 8 years ago. Breast ultrasound showed a nodule in lower outer quadrant of the right breast 6 days ago. MIP PET (**A**), transverse CT (**B**), and corresponding fused (**C**) images showed a complex cyst with hypermetabolic mural nodule (SUV_{max}, 3.3) in the right breast (arrows). The patient underwent resection of the lesion. Photomicrograph (**D**) revealed intraductal papilloma (hematoxylin-eosin stain; original magnification, ×200).

finding in DCIS is microcalcifications (Fig. 13). A finding of segmental or ductal nonmass-like enhancement at contrast enhanced MRI is a hallmark of DCIS.[39] Reports on FDG PET findings of DCIS are limited. The mean SUV_{max} of DCIS is approximately 2.0 to 2.4 (Fig. 13).[10,40] Avril et al found that the sensitivity of FDG PET in detecting DCIS is only 25%.[41] Mavi et al suggested that dual time point FDG PET was helpful for improving the detection of DCIS with sensitivity of 76.9% because of increasing of the contrast between the lesion and the surrounding background.[10] Compared with invasive carcinoma, DCIS shows lower intratumoral metabolic heterogeneity, which may be helpful for preoperative identification of invasive components in biopsy-confirmed DCIS.[40]

Invasive Ductal Carcinoma and Invasive Lobular Carcinoma

Invasive ductal carcinoma (IDC) is a heterogeneous group of tumors comprising the largest group (40%–70%) of invasive breast carcinomas.[31] Invasive lobular carcinoma (ILC) is the second most common breast carcinoma, accounting for 10% to 15% of invasive breast carcinomas.[31] The likelihood of bilaterality and multifocality of ILC is increased compared with IDCs. At CT, IDCs may be spiculated, rounded, occult, or other. They may show marked early and/or peripheral enhancement. Invasive lobular carcinoma spreads through the breast parenchyma by means of diffuse infiltration, which may cause little disruption of the underlying anatomical structures. CT findings of ILC may be nonspecific, showing an asymmetric soft-tissue density or a mass.[32]

Various cellular components and a variety of molecular mechanisms contribute to FDG uptake in breast carcinoma. The most important factors are expression of Glut-1 and hexokinase, number of viable tumor cells, histological subtype, microvessel density, tumor cell proliferation, and presence of inflammatory cells.[42] Larger tumors, high-grade tumors, and tumors with the triple-negative profile tend to have higher FDG uptake.[43,44] Estrogen receptor-negative tumors demonstrate a significantly higher SUV_{max} than do estrogen receptor-positive tumors.[45] Invasive lobular carcinomas demonstrate lower SUV_{max} than IDCs. The lower FDG uptake in ILC may account for decreased detection rates on FDG PET.[46] A lower tumor cell density, a diffuse infiltration of surrounding tissue, a low level of GLUT-1 expression, and a decreased proliferation rate in ILCs could explain this finding.[47] Osseous metastases in patients with ILC also demonstrate lower FDG avidity than those in IDC patients. The non-FDG-avid sclerotic osseous metastases are significantly more common in untreated patients with ILC than with IDC.[48] The impact of FDG PET/CT on systemic staging may be lower for ILC patients than for IDC patients.[49]

The specificity of PET for breast carcinoma detection is high, but sensitivity is relatively low. Avril et al showed that the specificity and sensitivity of single time point FDG PET in detecting invasive carcinoma is 94% and 62%, respectively.[41] Dual time imaging can improve the sensitivity of FDG PET for detecting small breast carcinoma. Mavi et al reported that the sensitivity of dual time FDG PET for detecting breast carcinomas with size of 4 to 10 mm reached as high as 82.7%.[10] Breast MRI has been increasingly adopted in clinical practice. It offers excellent sensitivity (90%) with relatively lower specificity (75%).[50] The combined information of FDG PET and

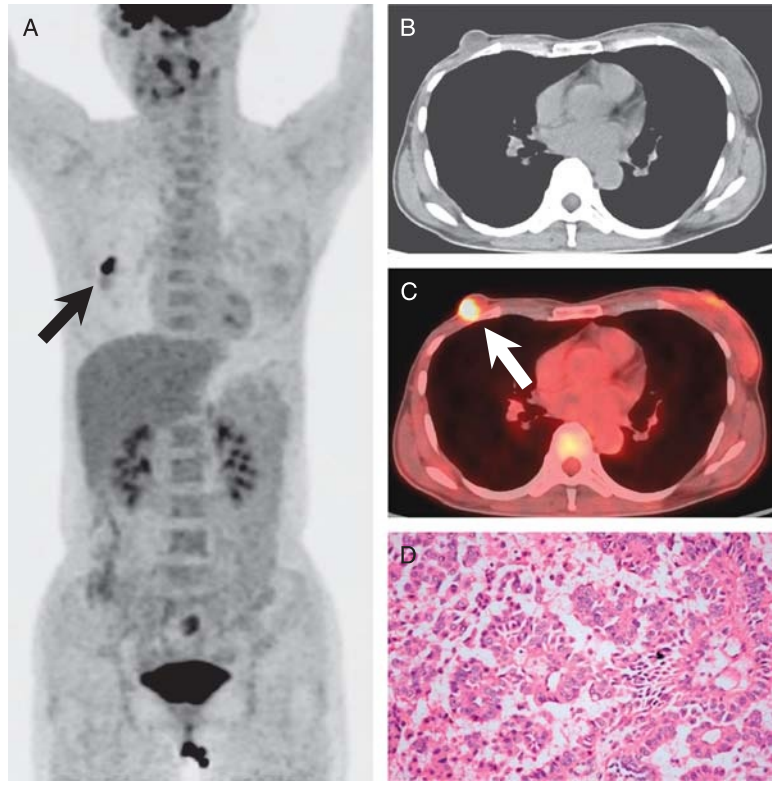

FIGURE 12. A 39-year-old woman who incidentally found a nodule adjacent to right nipple. She underwent right breast carcinoma resection 2 years ago. MIP PET (**A**), transverse CT (**B**), and corresponding fused (**C**) images showed a FDG-avid lesion with SUV_{max} of 10.1 in the right nipple (arrows). The patient underwent resection of the lesion. Photomicrograph (**D**) revealed intraductal papillary carcinoma (hematoxylin-eosin stain; original magnification, ×200).

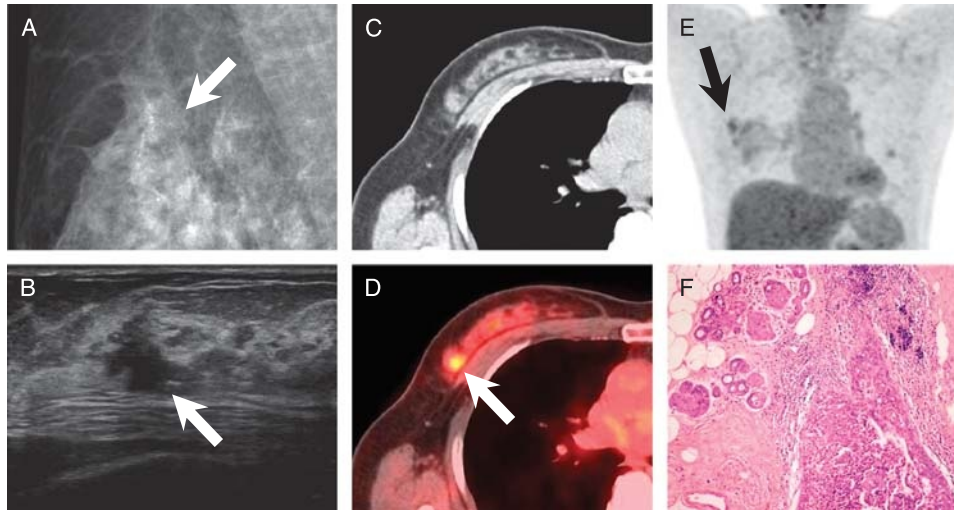

FIGURE 13. A 57-year-old woman who incidentally found a right breast nodule 2 months ago. Right mediolateral mammogram (**A**) showed an irregular nodule (arrow) with punctate microcalcifications in upper outer quadrant of the right breast. Breast ultrasound (**B**) showed an irregular-shaped hypoechoic nodule (arrow) measuring 1.7 × 1.2 cm with nonparallel orientation. Transverse CT (**C**), corresponding fused (**D**), and MIP PET (**E**) images showed a hypermetabolic nodule with SUV_{max} of 3 in the right breast (arrows). The patient underwent resection of the nodule. Photomicrograph (**F**) revealed ductal carcinoma in situ with lobular involvement (hematoxylin-eosin stain; original magnification, ×100). There were calcifications between the tumor cells.

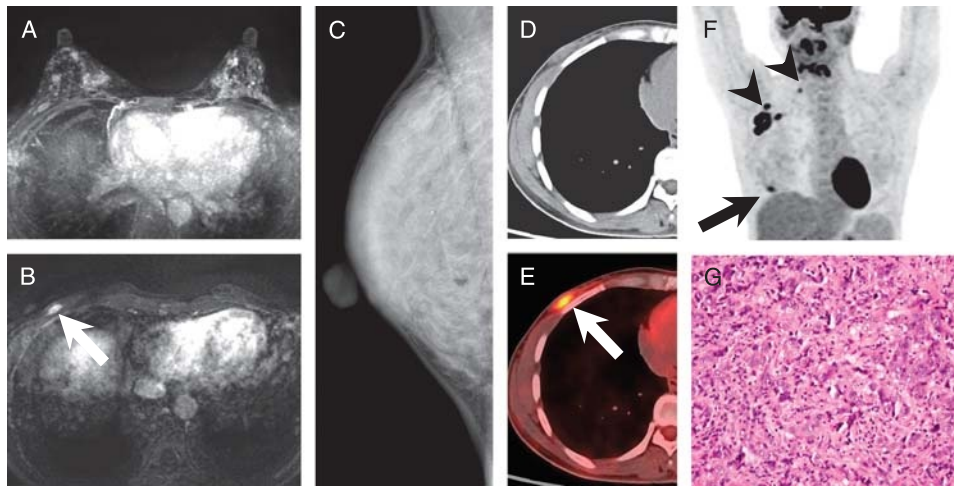

FIGURE 14. A 40-year-old woman who incidentally found a nodule in lower outer quadrant of the right breast 1 month ago. MIP-enhanced T1-weighted MR image (**A**) and transverse-enhanced T1-weighted MR image (**B**) showed multiple enhanced nodules of the bilateral breasts and cannot judged which one was malignant tumor. There were multiple enlarged lymph nodes in the right axilla (not shown). Right axillary lymph node metastasis was confirmed by biopsy. Right mediolateral mammogram (**C**) showed extremely dense breast. Transverse CT (**D**), corresponding fused (**E**), and MIP PET (**F**) images showed a FDG-avid lesion with SUV_{max} of 4.0 in lower outer quadrant of the right breast (arrows) corresponding to the enhanced nodule (arrow) in image B. There were ipsilateral axillary and superclavicular lymph node metastases (arrowheads). Photomicrograph (**G**) of the resected FDG-avid breast lesion revealed IDC (hematoxylin-eosin stain; original magnification, ×200).

MRI increases user's confidence in image interpretation in the specific case of patients with breast carcinoma (Fig. 14).[51]

Invasive Micropapillary Carcinoma

Invasive micropapillary carcinoma is composed of small clusters of tumor cells lying within clear stromal spaces resembling dilated vascular channels. Carcinomas with a dominant micropapillary growth pattern account for less than 2% of all invasive breast carcinomas.[31] This unusual growth pattern is correlated with the presence of vascular invasion and axillary lymph node metastases.

There is limited information about the radiological features of invasive micropapillary carcinoma of the breast. On MRI, it commonly shows irregular shape, spiculated margin, and heterogeneous enhancement and frequently shows multiple lesions.[52] We presented a case of invasive micropapillary carcinoma showing multiple lesions with inhomogeneous FDG uptake (Fig. 15).

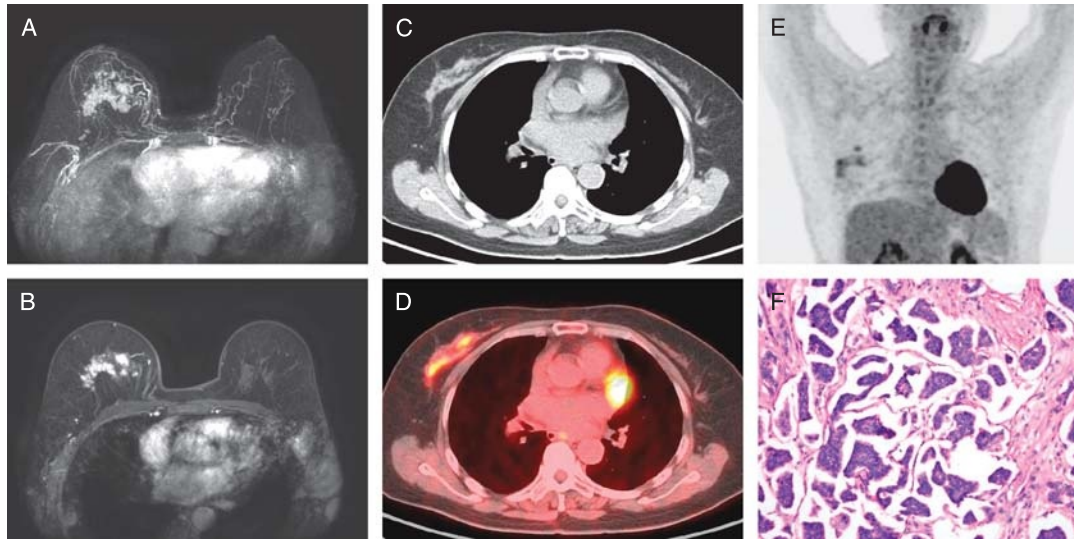

FIGURE 15. A 57-year-old woman with elevated carbohydrate antigen 19-9 for 2 months. MIP-enhanced T1-weighted MR (**A**) and transverse-enhanced T1-weighted MR images (**B**) showed multifocal nodules with remarkable enhancement in the right breast. Transverse CT (**C**), corresponding fused (**D**), and MIP PET (**E**) images showed inhomogeneous FDG uptake of right breast with SUV_{max} of 3.0. Photomicrograph (**F**) of the resected right breast specimen revealed invasive micropapillary carcinoma (hematoxylin-eosin stain; original magnification, ×200).

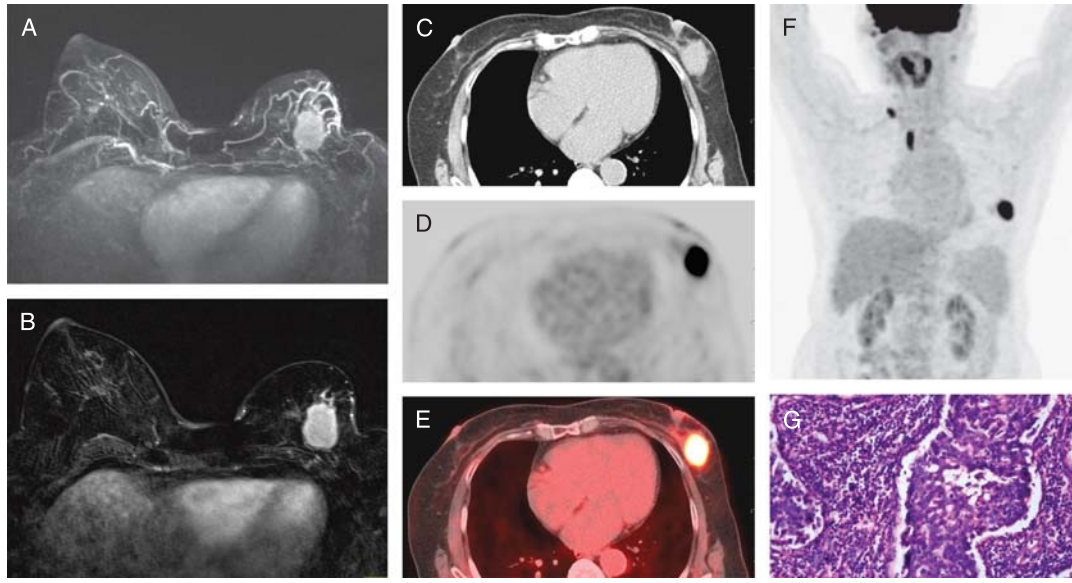

FIGURE 16. A 70-year-old woman who incidentally found a nodule in her left breast 1 month ago. MIP-enhanced T1-weighted MR (**A**) and transverse-enhanced T1-weighted MR images (**B**) showed an ovoid mass with rim enhancement in the left breast. Transverse CT (**C**), corresponding PET (**D**), fused (**E**), and MIP PET (**F**) images showed intense FDG uptake of the mass with SUV_{max} of 12.9 and FDG-avid lymph nodes in the mediastinal and right superaclavicular regions. Photomicrograph (**G**) of the resected mass revealed medullar carcinoma with prominent lymphoplasmacytic infiltrate (hematoxylin-eosin stain; original magnification, ×200).

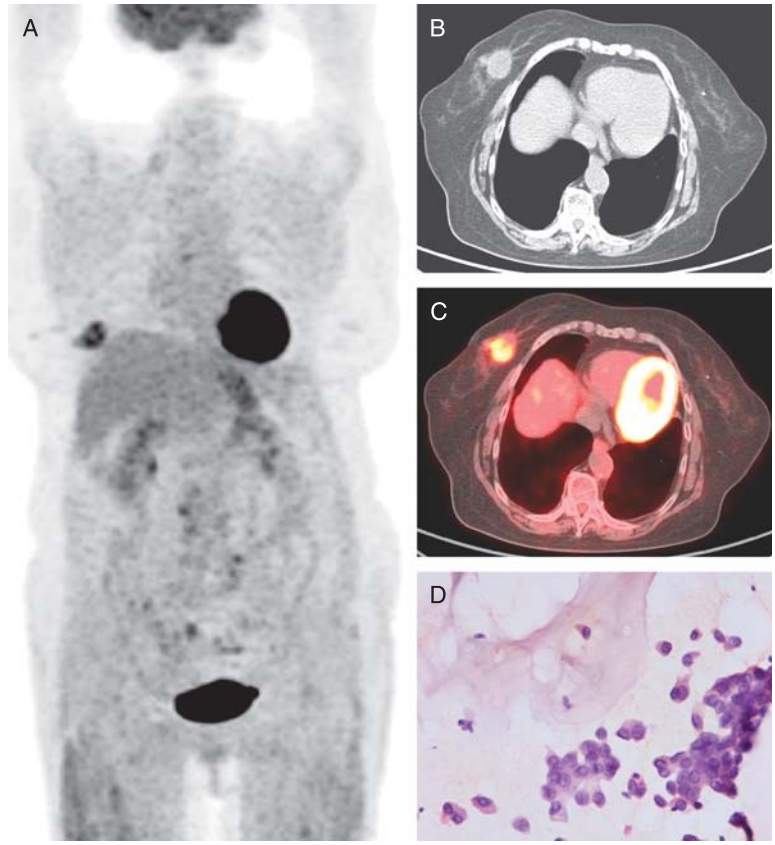

FIGURE 17. A 83-year-old woman with right breast pain for 2 weeks. MIP PET (**A**), transverse CT (**B**), and corresponding fused (**C**) images showed a hypermetabolic mass with SUV_{max} of 5.3. Fine needle aspiration of the mass revealed mucinous carcinoma with abundant mucinous matrix (**D**, hematoxylin-eosin stain; original magnification, ×200).

Medullary Carcinoma

Medullary carcinoma is a well-circumscribed carcinoma composed of poorly differentiated cells arranged in large sheets, with no glandular structures, scant stroma, and a prominent lymphoplasmacytic infiltrate. It represents between 1% and 7% of all breast carcinomas.[31] Medullary carcinoma has a better prognosis than the common invasive ductal carcinoma.

On MRI, the common features are an oval or lobular shape, a circumscribed margin, low apparent diffusion coefficient on diffusion-weighted imaging, rim enhancement, and washout or plateau pattern on kinetic curve.[53] On PET/CT, it can show intense FDG uptake, which may be due to high cellular density and prominent lymphoplasmacytic infiltrate (Fig. 16).[54,55]

Mucinous Carcinoma

Mucinous carcinoma is characterized by a proliferation of clusters of generally small and uniform cells floating in large amounts of extracellular mucus. Pure mucinous carcinoma accounts for approximately 2% of all breast carcinomas.[31] In general, pure mucinous carcinomas have a favorable prognosis.

The imaging features of mucinous carcinoma differ from those of common breast carcinomas because of its high extracellular water component (mucin pool) and relatively low cell density. MRI features of pure mucinous carcinoma include lobular shape, homogeneous strongly high signal intensity on fat suppressed T2-weighted images, high apparent diffusion coefficient on diffusion-weighted imaging, rim or heterogeneous enhancement, and persistent pattern on kinetic curve.[56,57] Mucinous carcinoma shows relatively lower FDG uptake, which may result from relatively low cellular density (Fig. 17).[10,55]

Metaplastic Carcinoma

Metaplastic carcinoma, a rare subtype accounting for less than 1% of invasive breast carcinomas, is characterized by high-grade carcinoma with heterogeneous metaplastic components.[31] Metaplastic carcinomas include pure epithelial (squamous cell, adenocarcinoma with spindle cell differentiation, or adenosquamous including mucoepidermoid) and mixed epithelial-mesenchymal (carcinoma with chondroid or osseous metaplasia, and carcinosarcoma).[31] They present with large tumors, aggressive pathological features, and frequent initial distant metastasis resulting in worse prognosis.[58]

At mammography, a metaplastic carcinoma typically is very dense and infrequently has calcifications. The MRI appearances of metaplastic carcinoma include a round or lobular mass with a relatively smooth margin, high signal intensity on T2-weighted images caused by the necrosis and cystic degeneration, rim-like enhancement, and washout pattern in the enhancing peripheral portion.[59] FDG PET/CT findings of metaplastic carcinomas are rare. Groheux et al have reported 7 patients with metaplastic carcinomas showing high $SUV_{max,}$ ranging from 6.2 to 18.9 (Fig. 18).[44] All the 7 tumors were grade 3, and 5 of them were triple negative. The status of p53 was found mutated in all cases. These factors may contribute to the high FDG uptake.

Lymphoma

Malignant lymphoma of the breast may present as a primary or secondary tumor; both are rare. Most breast lymphomas are B-cell lymphoma and, rarely, T-cell lymphoma. They present unilateral or bilateral breast involvement. They can show unifocal, multifocal, or diffuse FDG uptake. High-grade tumors intend to show

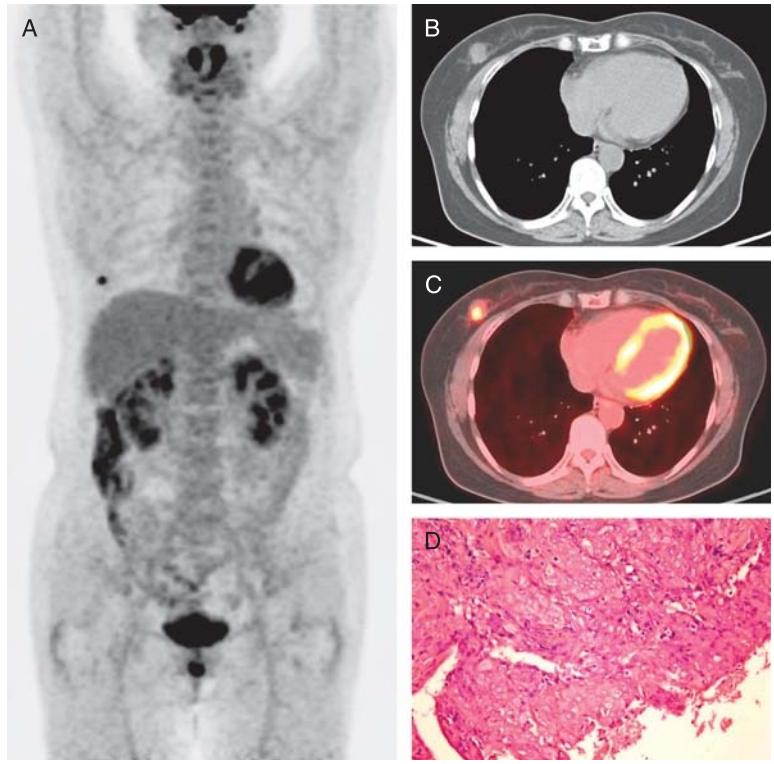

FIGURE 18. A 61-year-old woman who incidentally found a nodule in her right breast 2 weeks ago. MIP PET (**A**), transverse CT (**B**), and corresponding fused (**C**) images showed a FDG-avid nodule with SUV_{max} of 6.3 in the right breast. Photomicrograph (**D**) of the resected nodule revealed metaplastic squamous carcinoma (hematoxylin-eosin stain; original magnification, ×200).

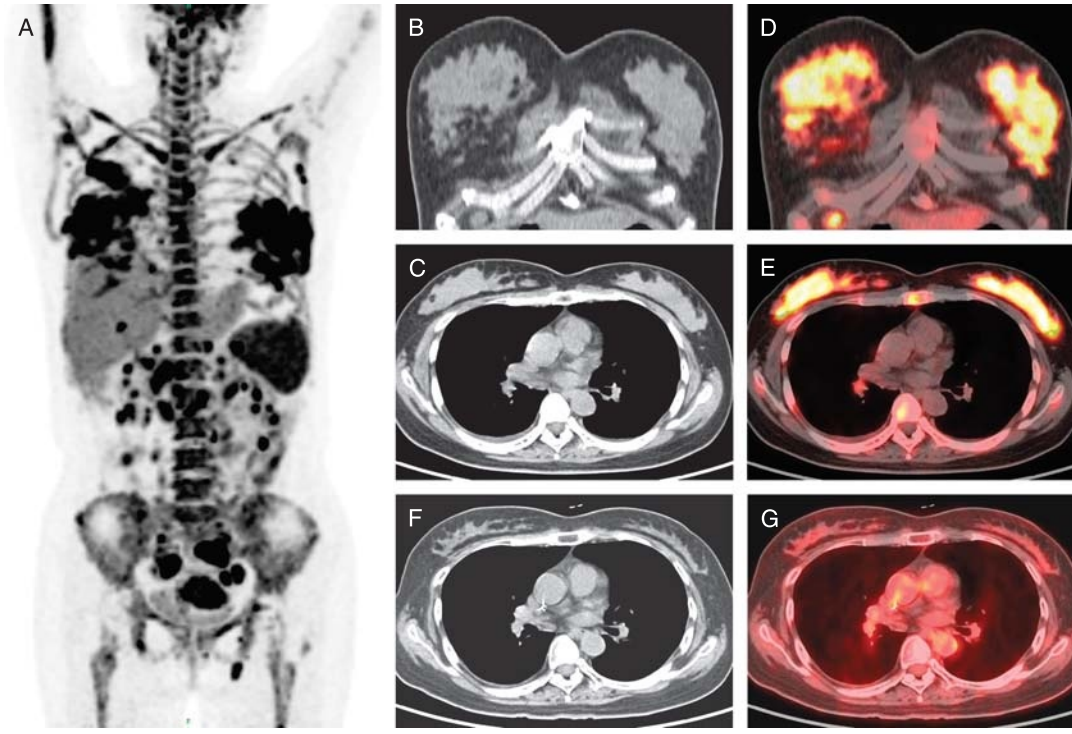

FIGURE 19. A 50-year-old woman who incidentally found bilateral breast masses 2 weeks ago. Breast biopsy revealed B-cell lymphoblastic leukemia/lymphoma. MIP PET (**A**), coronal (**B**) and transverse (**C**) CT, and corresponding fused (**D**, **E**) images showed enlargement of the bilateral breasts with diffuse FDG uptake ($SUV_{max,}$ 10.8). After 4 cycles of chemotherapy, a second FDG PET/CT was performed. Transverse CT (**F**) and corresponding fused (**G**) images showed regression of the breasts.

intense FDG uptake (Fig. 19).[60,61] Low-grade tumors, such as mucosa-associated lymphoid tissue lymphoma, show relatively lower activity.[62] Occasionally, breast lymphoma only involves breast skin and superficial tissue with high FDG uptake (Fig. 20).[63]

DISEASES OF THE MALE BREAST

Male breast disease encompasses a variety of benign and malignant conditions. Almost all tumors that occur in the female breast can occur in the male breast, although much more rarely.

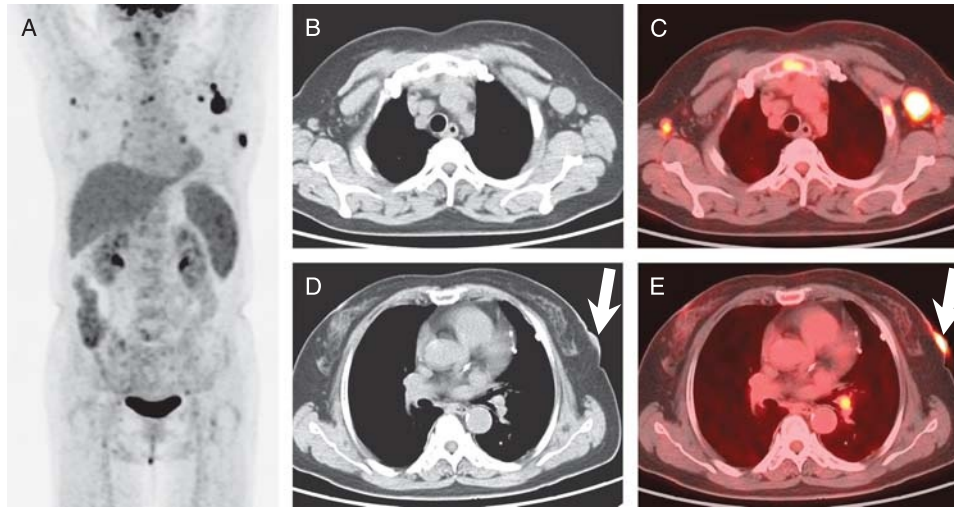

FIGURE 20. A 67-year-old woman with enlargement of bilateral axillary lymph nodes detected on CT 1 week ago. She underwent sigmoid colon carcinoma resection 1 year ago. MIP PET (**A**), transverse CT (**B**), and corresponding fused (**C**) images showed bilateral axillary FDG-avid lymph nodes. Transverse CT (**D**) and corresponding fused (**E**) images showed focally thickened skin (arrows) with intense FDG uptake (SUV_{max}, 18.5) in the left breast. The left breast skin was normal on CT 3 months ago (not shown). Left axillary lymph node biopsy revealed peripheral T-cell lymphoma.

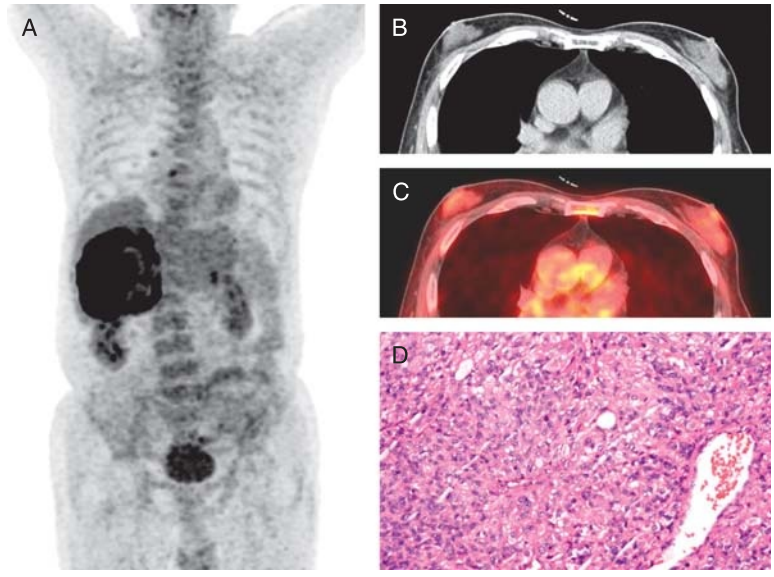

FIGURE 21. A 74-year-old man with incidental detection of right adrenal tumor on CT 2 months ago. Serum estradiol level was elevated (174 pg/mL). MIP PET (**A**) image showed a large FDG-avid tumor in right adrenal area. Transverse CT (**B**) and corresponding fused (**C**) images showed enlargement of bilateral breasts with increased FDG uptake. The patient underwent resection of right adrenal tumor. Photomicrograph (**D**) of the resected mass revealed adrenal cortical carcinoma (hematoxylin-eosin stain; original magnification, ×200).

Gynecomastia

Gynecomastia is the most common breast disease in men. It is a non-neoplastic, often reversible, enlargement of the rudimentary duct system in male breast tissue with proliferation of epithelial and mesenchymal components in response to hormonal stimulation. It may be unilateral or bilateral and is usually subareolar in location. In male subjects, estrogenic effects increase in neonates, adolescents, and the elderly. Additional risk factors for development of gynecomastia include estrogen-producing tumors of the testis, such as Sertoli or Leydig cell tumors; feminizing adrenal cortical tumors; gonadotropin-secreting tumors, such as hepatoblastoma and fibrolamellar carcinoma or choriocarcinoma; prolactinoma; liver disease; obesity; Klinefelter syndrome; testicular feminization syndrome; neurofibromatosis type 1; and medication use.[64,65]

On PET/CT, gynecomastia is visualized as increased volume of breast tissue on the CT. It usually shows FDG uptake lower than or similar to the liver background (Fig. 21).[66–68] Unilateral nodular gynecomastia with increased FDG uptake may mimic a primary or

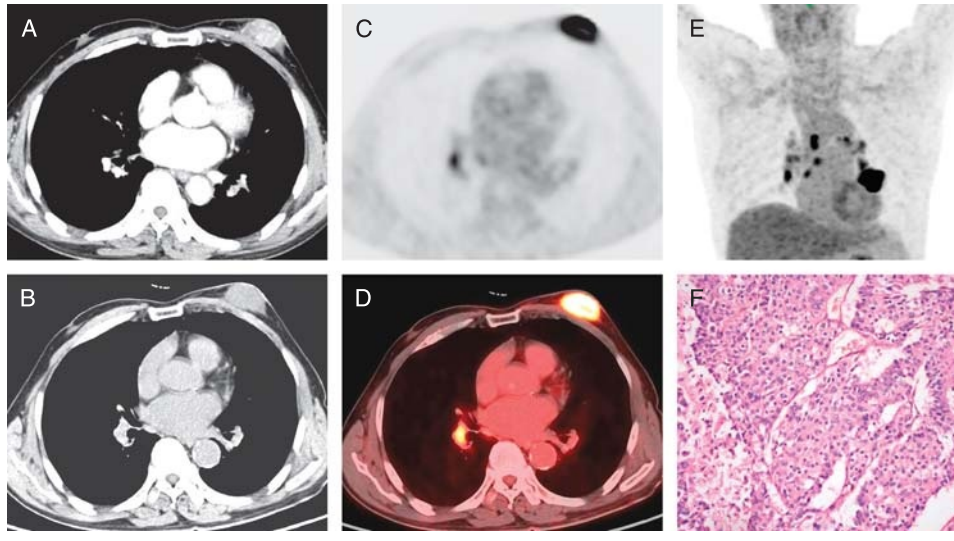

FIGURE 22. A 75-year-old man with a 10-year history of a left breast nodule. He found this nodule enlarged with pain 1 week ago. Chest transverse enhanced CT (**A**) showed a enhancing mass of the left breast. Transverse CT (**B**), corresponding PET (**C**), fused (**D**), and MIP PET (**E**) images showed strong FDG uptake of the mass with SUV_{max} of 28.5. Photomicrograph (**F**) of the resected mass revealed invasive breast carcinoma (hematoxylin-eosin stain; original magnification, ×200).

secondary tumor.[69] When interpreting FDG PET/CT as a staging tool in oncological male patients, one should consider gynecomastia as a possible cause for increased FDG uptake in the breast.

Male Breast Carcinoma

Carcinoma of the male breast is a rare malignant epithelial tumor histologically identical to that seen in the female breast. Male breast carcinoma is extremely rare, representing less than 1% of all breast carcinomas.[31] The relative lack of glandular activity in the male breast potentially increases the sensitivity of FDG PET/CT for detection of male breast cancer.[70,71] Groheux et al have reported that FDG PET/CT seems to be a powerful imaging method to perform staging, restaging, and treatment response assessment in male patients with breast carcinoma. They found that all the estrogen receptor positive breast carcinomas were FDG-avid (Fig. 22), and metastases could be detected with high sensitivity.[72]

CONCLUSIONS

It is difficult to distinguish true malignant breast lesions from benign ones on FDG PET/CT because there is significant overlap between the FDG-avidity of malignant and benign lesions on FDG PET, and CT is also poor for evaluation of lesions within the breast. In this atlas article, we demonstrate many representative lesions, which we have encountered, in an attempt to assist other interpreting physicians in expanding the differential diagnosis for hypermetabolic lesions in the breast.

REFERENCES

1. Rosen EL, Eubank WB, Mankoff DA. FDG PET, PET/CT, and breast cancer imaging. *Radiographics*. 2007;27:S215–S229.
2. Lim S, Lee EH, Park JM, et al. Role of combined BI-RADS assessment using mammography and sonography for evaluation of incidental hypermetabolic lesions in the breast on 18F-FDG PET-CT. *Acta Radiol*. 2013;54:1117–1124.
3. Shin KM, Kim HJ, Jung SJ, et al. Incidental breast lesions identified by (18)F-FDG PET/CT: which clinical variables differentiate between benign and malignant breast lesions? *J Breast Cancer*. 2015;18:73–79.
4. Kang BJ, Lee JH, Yoo IeR, et al. Clinical significance of incidental finding of focal activity in the breast at 18F-FDG PET/CT. *AJR Am J Roentgenol*. 2011;197:341–347.
5. Kumar R, Chauhan A, Zhuang H, et al. Standardized uptake values of normal breast tissue with 2-deoxy-2-[F-18]fluoro-D: −glucose positron emission tomography: variations with age, breast density, and menopausal status. *Mol Imaging Biol*. 2006;8:355–362.
6. Vranjesevic D, Schiepers C, Silverman DH, et al. Relationship between 18 F-FDG uptake and breast density in women with normal breast tissue. *J Nucl Med*. 2003;44:1238–1242.
7. Mavi A, Cermik TF, Urhan M, et al. The effect of age, menopausal state, and breast density on (18)F-FDG uptake in normal glandular breast tissue. *J Nucl Med*. 2010;51:347–352.
8. Lin CY, Ding HJ, Liu CS, et al. Correlation between the intensity of breast FDG uptake and menstrual cycle. *Acad Radiol*. 2007;14:940–944.
9. Park HH, Shin JY, Lee JY, et al. Discussion on the alteration of 18 F-FDG uptake by the breast according to the menstrual cycle in PET imaging. *Conf Proc IEEE Eng Med Biol Soc*. 2013;2013:2469–2472.
10. Mavi A, Urhan M, Yu JQ, et al. Dual time point 18 F-FDG PET imaging detects breast cancer with high sensitivity and correlates well with histologic subtypes. *J Nucl Med*. 2006;47:1440–1446.
11. Sabate JM, Clotet M, Torrubia S, et al. Radiologic evaluation of breast disorders related to pregnancy and lactation. Radiographics. 2007;27(Suppl 1):S101–S124.
12. Hsieh TC, Wu YC, Sun SS, et al. FDG PET/CT of a late-term pregnant woman with breast cancer. *Clin Nucl Med*. 2012;37:489–491.
13. Hicks RJ, Binns D, Stabin MG. Pattern of uptake and excretion of (18)F-FDG in the lactating breast. *J Nucl Med*. 2001;42:1238–1242.
14. Ko KH, Jung HK, Jeon TJ. Diffuse intense 18 F-FDG uptake at PET in unilateral breast related to breastfeeding practice. *Korean J Radiol*. 2013;14:400–402.
15. Camps M, Vilaro S, Testar X, et al. High and polarized expression of GLUT1 glucose transporters in epithelial cells from mammary gland: acute down-regulation of GLUT1 carriers by weaning. *Endocrinology*. 1994;134:924–934.
16. Kamal RM, Hamed ST, Salem DS. Classification of inflammatory breast disorders and step by step diagnosis. *Breast J*. 2009;15:367–380.
17. Benveniste AP, Yang W, Benveniste MF, et al. Benign breast lesions detected by positron emission tomography-computed tomography. *Eur J Radiol*. 2014;83:919–929.
18. Lim HS, Yoon W, Chung TW, et al. FDG PET/CT for the detection and evaluation of breast diseases: usefulness and limitations. *Radiographics* 2007; 27(suppl 1):S197-S213.
19. Adejolu M, Huo L, Rohren E, et al. False-positive lesions mimicking breast cancer on FDG PET and PET/CT. *AJR Am J Roentgenol*. 2012;198:W304–W314.
20. Choi EK, Oh JK, Chung YA. Herpes zoster mimicking breast cancer with axillary lymph node metastasis on PET/CT. *Clin Nucl Med*. 2015;40:572–573.
21. Cho YS, Chung DR, Choi JY, et al. 18F-FDG PET/CT in a case of parasite infection mimicking lung and breast malignancy. *Clin Nucl Med*. 2015;40:85–87.
22. Das CJ, Kumar R, Balakrishnan VB, et al. Disseminated tuberculosis masquerading as metastatic breast carcinoma on PET-CT. *Clin Nucl Med*. 2008;33:359–361.
23. Chen CJ, Lee BF, Yao WJ, et al. A false positive F-FDG PET/CT scan caused by breast silicone injection. *Korean J Radiol*. 2009;10:194–196.
24. Bakheet SM, Powe J, Kandil A, et al. F-18 FDG uptake in breast infection and inflammation. *Clin Nucl Med*. 2000;25:100–103.
25. Yang WT, Le-Petross HT, Macapinlac H, et al. Inflammatory breast cancer: PET/CT, MRI, mammography, and sonography findings. *Breast Cancer Res Treat*. 2008;109:417–426.
26. Tan PH, Lai LM, Carrington EV, et al. Fat necrosis of the breast—a review. *Breast*. 2006;15:313–318.
27. Dobbs NB, Latifi HR. Diffuse FDG uptake due to fat necrosis following transverse rectus abdominus myocutaneous (TRAM) flap reconstruction. *Clin Nucl Med*. 2013;38:652–654.
28. Ulaner GA, D'Andrea G, Cody HS 3rd. Breast implant foreign body reaction mimicking breast cancer recurrence on FDG PET/CT. *Clin Nucl Med*. 2013;38:480–481.
29. Akkas BE, Ucmak Vural G. Fat necrosis may mimic local recurrence of breast cancer in FDG PET/CT. *Rev Esp Med Nucl Imagen Mol*. 2013;32:105–106.
30. Dupont WD, Page DL. Risk factors for breast cancer in women with proliferative breast disease. *N Engl J Med*. 1985;312:146–151.
31. Ellis IO, Schnitt SJ, Sastre-Garau X. Invasive breast carcinoma. In: Tavassoli F, Devilee P, eds. *World Health Organization classification of tumours: pathology and genetics of tumours of the breast and female genital organs*. Lyon, France: IARC; 2003:13–59.
32. Harish MG, Konda SD, MacMahon H, et al. Breast lesions incidentally detected with CT: what the general radiologist needs to know. *Radiographics*. 2007;27:S37–S51.
33. Yamaguchi R, Futamata Y, Yoshimura F, et al. Mastopathic-type fibroadenoma and ductal adenoma of the breast with false-positive fluorodeoxyglucose positron emission tomography. *Jpn J Radiol*. 2009;27:280–284.
34. Makis W, Ciarallo A, Hickeson M, et al. Rapidly growing complex fibroadenoma with surrounding ductal hyperplasia mimics breast malignancy on serial F-18 FDG PET/CT imaging. *Clin Nucl Med*. 2011;36:576–579.
35. Eiada R, Chong J, Kulkarni S, et al. Papillary lesions of the breast: MRI, ultrasound, and mammographic appearances. *AJR Am J Roentgenol*. 2012;198:264–271.
36. Nguyen BD, Lidner TK. Intraductal papilloma of the breast: F-18 FDG PET demonstration. *Clin Nucl Med*. 2005;30:481–482.
37. Hirose Y, Kaida H, Ishibashi M, et al. Glucose transporter expression of intraductal papilloma of the breast detected by fluorodeoxyglucose positron emission tomography. *Jpn J Radiol*. 2011;29:217–221.
38. Jinguji M, Kajiya Y, Nakajo M, et al. A case of intraductal papilloma of the breast with high 18 F-FDG uptake on PET/CT. *Clin Nucl Med*. 2015;40:905–907.
39. Yamada T, Mori N, Watanabe M, et al. Radiologic-pathologic correlation of ductal carcinoma in situ. *Radiographics*. 2010;30:1183–1198.

40. Yoon HJ, Kim Y, Kim BS. Intratumoral metabolic heterogeneity predicts invasive components in breast ductal carcinoma in situ. *Eur Radiol*. 2015;25:3648–3658.
41. Avril N, Rose CA, Schelling M, et al. Breast imaging with positron emission tomography and fluorine-18 fluorodeoxyglucose: use and limitations. *J Clin Oncol*. 2000;18:3495–3502.
42. Buck AK, Schirrmeister H, Mattfeldt T, et al. Biological characterisation of breast cancer by means of PET. *Eur J Nucl Med Mol Imaging*. 2004;31:S80–S87.
43. Kumar R, Chauhan A, Zhuang H, et al. Clinicopathologic factors associated with false negative FDG-PET in primary breast cancer. *Breast Cancer Res Treat*. 2006;98:267–274.
44. Groheux D, Giacchetti S, Moretti JL, et al. Correlation of high 18 F-FDG uptake to clinical, pathological and biological prognostic factors in breast cancer. *Eur J Nucl Med Mol Imaging*. 2011;38:426–435.
45. Osborne JR, Port E, Gonen M, et al. 18 F-FDG PET of locally invasive breast cancer and association of estrogen receptor status with standardized uptake value: microarray and immunohistochemical analysis. *J Nucl Med*. 2010;51:543–550.
46. Jung NY, Kim SH, Kim SH, et al. Effectiveness of breast MRI and (18)F-FDG PET/CT for the preoperative staging of invasive lobular carcinoma versus ductal carcinoma. *J Breast Cancer*. 2015;18:63–72.
47. Bos R, van Der Hoeven JJ, van Der Wall E, et al. Biologic correlates of (18) fluorodeoxyglucose uptake in human breast cancer measured by positron emission tomography. *J Clin Oncol*. 2002;20:379–387.
48. Dashevsky BZ, Goldman DA, Parsons M, et al. Appearance of untreated bone metastases from breast cancer on FDG PET/CT: importance of histologic subtype. *Eur J Nucl Med Mol Imaging*. 2015;42:1666–1673.
49. Hogan MP, Goldman DA, Dashevsky B, et al. Comparison of 18 F-FDG PET/CT for systemic staging of newly diagnosed invasive lobular carcinoma versus invasive ductal carcinoma. *J Nucl Med*. 2015;56:1674–1680.
50. Medeiros LR, Duarte CS, Rosa DD, et al. Accuracy of magnetic resonance in suspicious breast lesions: a systematic quantitative review and meta-analysis. *Breast Cancer Res Treat*. 2011;126:273–285.
51. Tabouret-Viaud C, Botsikas D, Delattre BM, et al. PET/MR in breast cancer. *Semin Nucl Med*. 2015;45:304–321.
52. Lim HS, Kuzmiak CM, Jeong SI, et al. Invasive micropapillary carcinoma of the breast: MR imaging findings. *Korean J Radiol*. 2013;14:551–558.
53. Jeong SJ, Lim HS, Lee JS, et al. Medullary carcinoma of the breast: MRI findings. *AJR Am J Roentgenol*. 2012;198:W482–W487.
54. Buck A, Schirrmeister H, Kühn T, et al. FDG uptake in breast cancer: correlation with biological and clinical prognostic parameters. *Eur J Nucl Med Mol Imaging*. 2002;29:1317–1323.
55. Baba S, Isoda T, Maruoka Y, et al. Diagnostic and prognostic value of pretreatment SUV in 18 F-FDG/PET in breast cancer: comparison with apparent diffusion coefficient from diffusion-weighted MR imaging. *J Nucl Med*. 2014;55:736–742.
56. Okafuji T, Yabuuchi H, Sakai S, et al. MR imaging features of pure mucinous carcinoma of the breast. *Eur J Radiol*. 2006;60:405–413.
57. Zhang L, Jia N, Han L, et al. Comparative analysis of imaging and pathology features of mucinous carcinoma of the breast. *Clin Breast Cancer*. 2015;15:e147–e154.
58. Jung SY, Kim HY, Nam BH, et al. Worse prognosis of metaplastic breast cancer patients than other patients with triple-negative breast cancer. *Breast Cancer Res Treat*. 2010;120:627–637.
59. Yoo JL, Woo OH, Kim YK, et al. Can MR Imaging contribute in characterizing well-circumscribed breast carcinomas? *Radiographics*. 2010;30:1689–1702.
60. Santra A, Kumar R, Reddy R, et al. FDG PET-CT in the management of primary breast lymphoma. *Clin Nucl Med*. 2009;34:848–853.
61. Yang WT, Lane DL, Le-Petross HT, et al. Breast lymphoma: imaging findings of 32 tumors in 27 patients. *Radiology*. 2007;245:692–702.
62. Kim DH, Jeong JY, Lee SW, et al. 18 F-FDG PET/CT finding of bilateral primary breast mucosa-associated lymphoid tissue lymphoma. *Clin Nucl Med*. 2015;40:e148–e149.
63. Schramm N, Pfluger T, Reiser MF, et al. Subcutaneous panniculitis-like T-cell lymphoma with breast involvement: functional and morphological imaging findings. *Br J Radiol*. 2010;83:e90–e94.
64. Lattin GE Jr, Jesinger RA, Mattu R, et al. From the radiologic pathology archives: diseases of the male breast: radiologic-pathologic correlation. *Radiographics*. 2013;33:461–489.
65. Chung EM, Cube R, Hall GJ, et al. From the archives of the AFIP: breast masses in children and adolescents: radiologic-pathologic correlation. *Radiographics*. 2009;29:907–931.
66. Fukuchi K, Sasaki H, Yokoya T, et al. Ga-67 citrate and F-18 FDG uptake in spironolactone-induced gynecomastia. *Clin Nucl Med*. 2005;30:105–106.
67. Wu YC, Hsieh TC, Sun SS, et al. Bilateral breast uptake demonstrated on FDG PET/CT scans in 3 male patients with hepatocellular carcinomas. *Clin Nucl Med*. 2012;37:520–521.
68. Wang HY, Jeng LB, Lin MC, et al. 18 F-FDG PET/CT in detection of gynecomastia in patients with hepatocellular carcinoma. *Clin Imaging*. 2013;37:942–946.
69. Ramtahalsing R, Arens AI, Vliegen RF, et al. False positive 18 F-FDG PET/CT due to gynaecomastia. *Eur J Nucl Med Mol Imaging*. 2007;34:614.
70. Sarma M, Borde C, Subramanyam P, et al. Random synchronous malignancy in male breast: a case report. *J Breast Cancer*. 2013;16:442–446.
71. McEachen JC, Kuo PH. Male primary breast cancer found on FDG-PET/CT. *Clin Nucl Med*. 2008;33:630–632.
72. Groheux D, Hindié E, Marty M, et al. ^{18}F-FDG-PET/CT in staging, restaging, and treatment response assessment of male breast cancer. *Eur J Radiol*. 2014;83:1925–1933.